LAAS Monitoring For A Most Evil Satellite Failure

Alexander M. Mitelman, Jaewoo Jung, Per K. Enge
Stanford University

BIOGRAPHY

Alexander Mitelman is a Ph.D. candidate in the Department of Electrical Engineering at Stanford University. As a member of the GPS Laboratory, his research is focused on local area differential GPS design, signal analysis and application. Mr. Mitelman received his S.B. in electrical engineering from the Massachusetts Institute of Technology in 1993 and his M.S. in electrical engineering from Stanford University in 1995.

Jaewoo Jung is a Ph.D. candidate in the Department of Aeronautics and Astronautics at Stanford University. His research is focused on local area differential GPS system design, analysis and application. Mr. Jung received his B.S. in aeronautics and astronautics from from Boston University in 1992 and his M.S. in aeronautics and astronautics from Stanford University in 1994.

Dr. Per Enge is an Associate Professor in the Department of Aeronautics and Astronautics at Stanford University. He received his B.S. in electrical engineering from the University of Massachusetts at Amherst in 1975, and his M.S. and Ph.D., both in electrical engineering, from the University of Illinois at Urbana-Champaign in 1979 and 1983. Professor Enge's research focuses on the design of navigation systems which satisfy stringent requirements with respect to accuracy, integrity (truthfulness), time availability, and continuity.

ABSTRACT

The objective of Signal Quality Monitoring (SQM) is to improve integrity of the space segment of Local Area Augmentation System (LAAS) by detecting satellite generated GPS signal faults. As seen in the SV19 case, these signal faults are particularly worrisome since pseudorange error may not be common mode between ground and air. This can render the differential correction ineffective, possibly leading to hazardously misleading information (HMI) being supplied to the aircraft.

The susceptibility of a differential architecture to such satellite faults is primarily due to the use of non-identical receivers on the ground and in the air. While the correlator spacings in aircraft receivers vary widely, most reference stations use narrow correlators to limit the effects of ground-based multipath. For this reason, air and ground correlator spacings are, in general, unequal. This leads to the possibility that a signal could appear to be nominally correct on the ground while generating a significant error at the aircraft.

To address the problem, this paper explores the use of one or more additional correlator sample pairs, or monitors, at the reference station to put a finite bound on the worst-case mismatch between ground and air estimates of the code phase. A mathematical model of the reference station is used to derive an explicit worst-case waveform for all possible combinations of air and ground correlator spacings as a function of M, the number of monitors. A simplified fault model using only the nominal GPS signal plus scaled, delayed copies of that signal, is also analyzed.

INTRODUCTION

The Global Positioning System offers a robust source of three-dimensional position information. Thanks to its versatility, GPS is finding increasingly widespread use in civil applications. One application of current interest is the Local Area Augmentation System (LAAS), in which a ground reference station provides differential corrections to airborne users for local navigation, precision approach and landing. A detailed description of the LAAS architecture is presented in [1].

As with any safety-of-life system, the LAAS must meet strict specifications on integrity, availability and continuity

if it is to be used for landing aircraft. In some cases, these specifications lead to conflicting requirements, and meeting them simultaneously is a major challenge facing system designers today. In particular, the LAAS must be able to correctly detect and flag any condition which would cause hazardously misleading information (HMI) to be broadcast to airborne users within 2 seconds (the specified time-to-alarm). On the other hand, the system must not be so conservative as to signal alarms in response to minor, non-hazardous interruptions, as this would lead to unacceptably low system continuity. These requirements are the primary motivation for Signal Quality Monitor (SQM) within the LAAS architecture.

FAULT DETECTION

Potentially hazardous signal faults may occur in the space, ground, or user segments of GPS; in this paper, we concentrate on those faults which could originate in the space segment. To date, a number of SV-based anomalies have been reported in the literature. A corrupted C/A code spectrum was observed on a healthy satellite in [2]. A transient code outage (later found to be associated with software uploads for Block II satellites) was reported in [3]. A clock event which caused L_1 carrier and C/A code range rates to exceed the Selective Availability NTE specifications for velocity and acceleration was observed in [4].

To detect faults of this type, we propose a monitoring strategy which involves a modification of the nominal architecture of the LAAS ground reference station. Currently, the reference station uses a single narrow correlator (typically a 0.1-chip spacing) to calculate corrections. We define a *monitor* to be an additional correlator used by the ground station to infer more detailed information about an underlying correlation peak than would be available from the reference correlator alone. By sampling the peak in multiple places, it is possible to detect asymmetries and other distortions which may go unnoticed in the non-monitored case.

A SIMPLIFIED FAULT MODEL

In this section we explore a simplified fault model which is mathematically straightforward and has a physically plausible origin. In the absence of a specific fault mode hypothesis, consider a GPS signal consisting of a nominal C/A code along with one or more scaled, delayed copies of that signal. This may be expressed mathematically as

$$s(t) = s_0(t) + \sum_{k=1}^{N} m_k\, s_0(t - \tau_k) \qquad (1)$$

where $s_0(t)$ is the nominal C/A code and m_k and τ_k are the relative amplitude and delay of the kth echo, respectively. Note that this expression may, in general, be used to model ground-based multipath as well as anomalies originating on the satellite. The ground reference station can distinguish between the two, however, by determining whether the interference appears on only one channel (which would suggest an SV-generated fault) or on several channels (which would indicate ground-based multipath or some other common-mode error source).

The correlation peak for the $N = 1$ case is shown in Figure 1. The thin solid line is the nominal peak with no interference; the dashed line is the echo; and the heavy solid line is the composite peak, which is what a correlator actually receives.

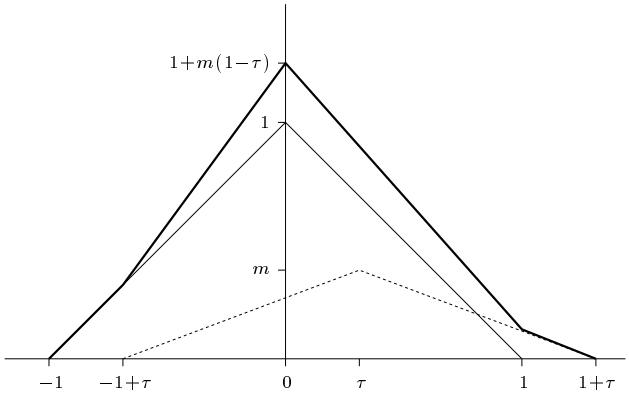

Figure 1: Simple reflection case (with $N = 1$)

A special case of Equation 1, described by $m_k = (m_0)^k$ and $\tau_k = \tau_{\mathrm{RT}}$, can be used to model of a misterminated transmission line. Rapid environmental changes, mechanical component failure and aging of electronic parts could all lead to this type failure mode, which is not uncommon in radio frequency (RF) applications involving transmission lines. In this case, the series of echos decreases geometrically in amplitude and arrives in integer multiples of the round-trip time.

For the single-reflection case shown in Figure 1, it is possible to derive a function, $\hat{\tau}(\alpha)$, which gives the code phase estimate as a function of the correlator width. This function takes the following form:

For $m > 2\tau - 1$,

$$\hat{\tau}(\alpha) = \begin{cases} \alpha m & 0 < \alpha \le \frac{\tau}{m+1} \\ \frac{m\tau}{m+1} & \frac{\tau}{m+1} < \alpha \le 1 - \frac{\tau}{m+1} \\ \frac{m(\tau+1-\alpha)}{m+2} & 1 - \frac{\tau}{m+1} < \alpha \le 1 - \frac{m\tau}{2} \\ \frac{m\tau+(m-1)(1-\alpha)}{m+1} & 1 - \frac{m\tau}{2} < \alpha \le 1 + \frac{\tau}{2} \end{cases} \qquad (2)$$

and for $m \leq 2\tau - 1$,

$$\hat{\tau}(\alpha) = \begin{cases} \alpha m & 0 < \alpha \leq \frac{\tau-1}{m-1} \\ \frac{m(\tau-1-\alpha)}{m-2} & \frac{\tau-1}{m-1} < \alpha \leq \tau - \frac{m}{2} \\ \frac{m(\tau+1-\alpha)}{m+2} & \tau - \frac{m}{2} < \alpha \leq 1 - \frac{m\tau}{2} \\ \frac{m\tau+(m-1)(1-\alpha)}{m+1} & 1 - \frac{m\tau}{2} < \alpha \leq 1 + \frac{\tau}{2} \end{cases} \quad (3)$$

These expressions can be used to predict the behavior of a given correlator in terms of its spacing and the signal parameters. Those values, in turn, can be used to estimate differential correction errors between ground an air. For a typical LAAS ground station with one monitor, the simplest decision statistic is defined as

$$DS = \hat{\tau}(\alpha_{\text{mon}}) - \hat{\tau}(\alpha_{\text{ref}}) \quad (4)$$

Combining equations 2 and 3, the analysis suggests that DS will bound the differential error at the aircraft provided $\alpha_{\text{mon}} > \alpha_{\text{air}} > \alpha_{\text{ref}}$. In other words, as long as the aircraft uses a spacing between that of the reference and that of the monitor, DS provides a meaningful metric on the integrity of the differential corrections.

This result was verified by simulation in Matlab. Figure 2 shows five runs of the single-reflection case with reflection amplitude $m = 0.5$, ground spacings $\alpha_{\text{mon}} = 0.5$, $\alpha_{\text{ref}} = 0.1$ and air spacings at $\alpha_{\text{air}} = \{0.2, 0.3, 0.5, 0.7, 0.8\}$ (all values are expressed in chips). The echo delay, τ, is the parameter in each plot and is swept from 0 to 1 chip. Indeed,

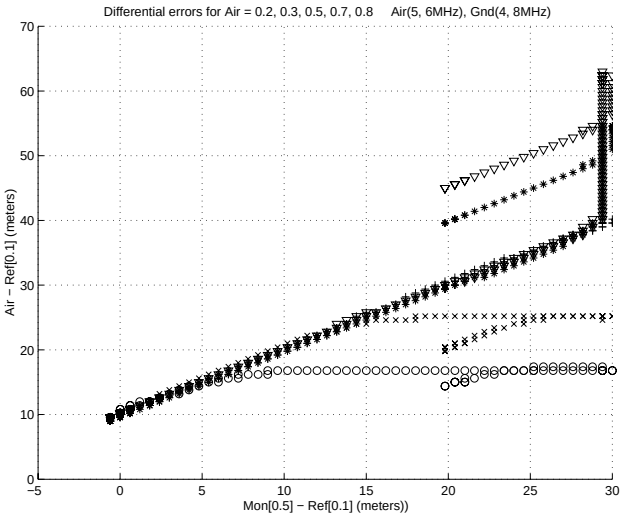

Figure 2: Aircraft error vs. decision statistic ($N = 1$)

the traces corresponding to air spacings of 0.2 (o) and 0.3 (x), lie below the line bounded by D, while those corresponding to air spacings outside the monitor lie above this line. Therefore it appears that the analytical expressions in equations 2 and 3 are an accurate representation of the single-reflection case.

Unfortunately the foregoing analysis represents the limit of what can be worked easily by hand. For multiple reflections ($N \geq 2$) or multiple monitors ($M \geq 2$), the analysis rapidly becomes intractable and computer simulation is needed. Defining a decision statistic also becomes an important issue, as there is no longer a single, unambiguous way to combine the information obtained from the monitors. In particular, a decision statistic may take the form $f(\mathbf{M}) = f(m_1, m_2, \ldots, m_M)$ The key is finding an explicit function which offers the tightest possible bound on differential error, subject to the competing constraints on integrity and availability described previously. Candidate decision statistics include

$$\begin{aligned} DS_{\max} &= \max_{m=1\ldots M} (\hat{\tau}(\alpha_{\text{m}}) - \hat{\tau}(\alpha_{\text{ref}})) \\ DS_{\text{avg}} &= \sum_{m=1}^{M} (\hat{\tau}(\alpha_{\text{m}}) - \hat{\tau}(\alpha_{\text{ref}})) \\ DS_{\text{poly}} &= \sum_{m=1}^{M} \beta_m (\hat{\tau}(\alpha_{\text{m}}) - \hat{\tau}(\alpha_{\text{ref}}))^{\gamma_m} \end{aligned}$$

which represent maximum monitor error, mean monitor error and a polynomial weighting, respectively. Further analysis and optimization of these candidate functions is the logical next step in this analysis.

A GENERAL FAULT MODEL

The preceding section postulates a simple fault model which has a plausible physical origin and is tractable analytically. In this section, we derive a *generalized* fault model and calculate the worst possible error which could pass undetected through a given configuration of air, reference and monitor correlators.

Consider a nominal GPS signal (C/A code and carrier) on L_1 with some arbitrary interference:

$$c(t) = \sqrt{2C_X}\, d(t-\tau) x(t-\tau) \cos(2\pi f_{L_1} t + \phi) + j(t) \quad (5)$$

where $j(t)$ has power spectral density $J(f)$. We define the *most evil waveform* (MEW) as the input $j(t)$ which maximizes the differential error between the user and the reference station. In general, $j(t)$ is a function of the system parameters (correlator spacings, filters, etc.).

To derive this waveform, we start by considering a single integrator-accumulator block and its frequency domain equivalent, as shown in Figure 3. The output of this block is precisely equivalent to a single correlator sample, and the frequency domain representation is called a *matched filter* for the replica signal $x(t)$.

A pair of matched filters with suitably time-shifted replicas may be combined to form an early-late correlator of the

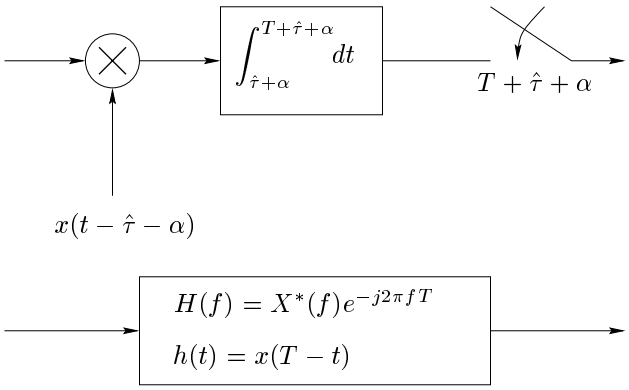

Figure 3: Single integrator-accumulator model

type used in most GPS receivers. This system is shown in Figure 4. (The sinusoidal term in the frequency domain representation arises from the difference of two complex exponentials.)

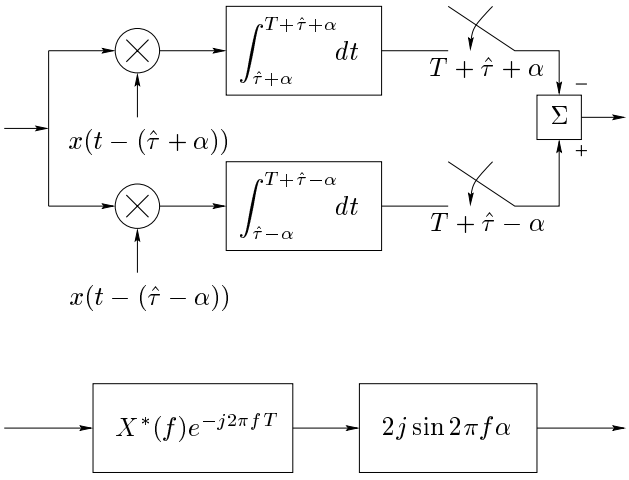

Figure 4: Early-late correlator model

Next, a basic differential system may be modeled by extending the ideas of Figure 4 to include two different correlator spacings, as shown in Figure 5. From the definition above, $j(t)$ is the input which maximizes $z_a(t)$, the differential error at the aircraft. This input is effectively matched to the overall transfer function, and is evidently a function of the correlator spacings on the ground and in the air.

Finally, the most general model is shown in Figure 6. This represents a general LAAS with an arbitrary number of monitors. The heavy dashed line encloses all the processing done at the reference station; this is the raw data upon which candidate SQM algorithms operate. From this model it is possible to solve for the specific worst-case waveform, $j(t)$, for a given configuration of monitors. Each of the monitors may be expressed as a frequency-domain function of the form

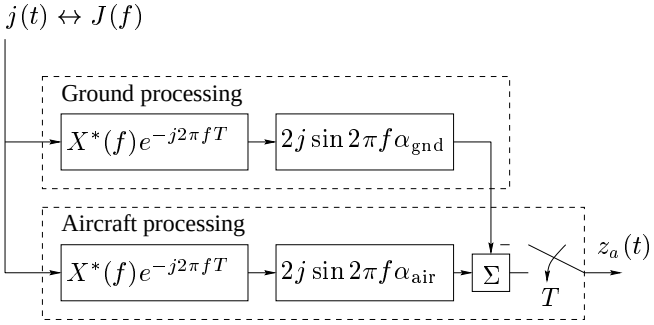

Figure 5: A basic LAAS with no monitors ($M = 0$)

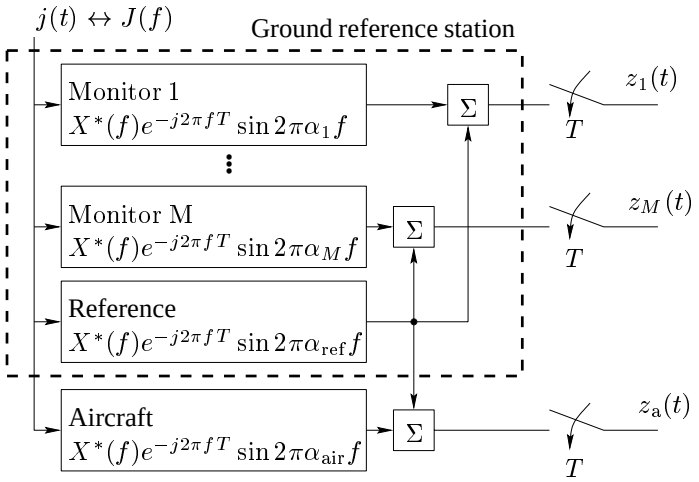

Figure 6: A general LAAS with monitors ($M \geq 1$)

$$Y^k_{\text{mon}}(f) = 2jX^*(f)e^{-j2\pi fT}\sin 2\pi f\alpha^k_{\text{mon}} \qquad (6)$$

The reference correlator, $Y_{\text{ref}}(f)$, and the aircraft correlator, $Y_{\text{air}}(f)$ are expressed in a similar fashion. Starting with these functions, we construct $J(f)$ (and, through the inverse Fourier transform, $j(t)$) by applying the Schwartz inequality to a procedure known as *Gram-Schmidt orthogonalization*. As the name suggests, this procedure yields a function which is orthogonal to each of the monitor functions (*i.e.*, it yields zero error at those sample points), but whose inner product with the air function $Y_{\text{air}}(f)$ is maximum. Put another way, $j(t)$ yields a cross-correlation peak which is *indistinguishable from a nominally clean peak at every monitor spacing*, but maximally asymmetric at a particular air spacing, subject to the constraint that the total energy in the evil waveform is equal to that in a nominal code chip. For example, the orthogonalization for $M = 1$ is:

$$J_1(f) = Y^*_{\text{air}}(f) - \frac{\langle Y^*_{\text{air}}, Y^1_{\text{mon}}\rangle}{|Y^1_{\text{mon}}|^2} Y^1_{\text{mon}}(f) \qquad (7)$$

where $\langle\cdot\rangle$ denotes the inner product.

The results of this analysis are presented in the next section.

More comprehensive treatments of the Gram-Schmidt process are given in [5] and [6].

RESULTS

In this section we present some results of the MEW analysis. First, Figure 7 shows the worst-case errors for three monitoring strategies – one, two and six monitors. As expected, the introduction of additional monitors confines the worst-case undetectable error to smaller and smaller values.

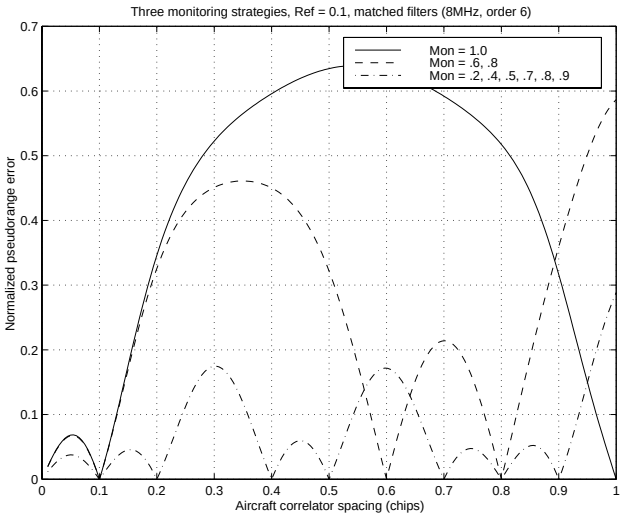

Figure 7: Three monitoring strategies ($M = 1, 2, 6$)

An informative, if impractical, result is shown in Figure 8, which illustrates the effects of placing a very large number (42 in this case) of monitors on a correlation peak. The largest error for any aircraft spacing in between the reference at 0.2 chips and 1 chip is on the order of $5-10\mu$m! Of course, this example is not physically useful because such a system would have virtually no continuity due to thermal noise-induced false alarms. Still, the effect is clear: additional monitors reduce the worst-case undetectable error.

Finally, Figure 9 suggests an interesting direction for future work. One thousand trials were run with each number of monitors shown and the monitors were randomly distributed between 0.05 and 1 chip for each trial. The worst-case error was computed and stored for each trial, and the *smallest* worst-case error was tracked throughout the simulation. Presumably, the smallest worst-case error for each value of M was generated by a near-optimal monitoring strategy for M monitors. The simulation suggests that uniform spacing is very nearly (but not quite) optimal for $M \geq 2$! (For $M = 1$, however, the optimal spacing appears to be slightly less than 1 chip apart.) This result

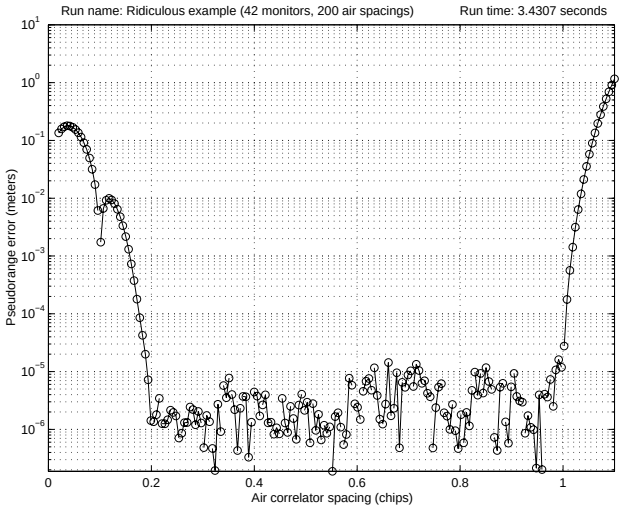

Figure 8: Ridiculous example ($M = 42$)

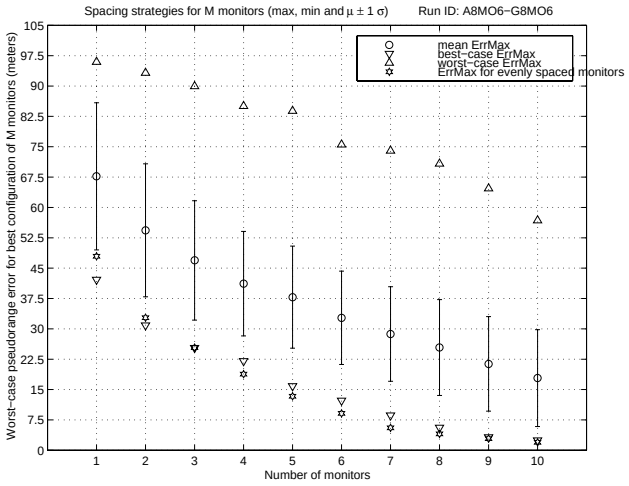

Figure 9: Optimal monitoring strategies

suggests an interesting optimization problem in M – what is the optimal way to place monitors?

The results of the MEW analysis are useful in several ways. First, it is straightforward to compute an absolute worst-case error bound for a particular monitoring strategy, without having to know anything at all about the explicit form of any potential signal anomaly. Second, the worst-case error for a given system is dependent both on the number of monitors and their placement; therefore this analysis offers a tool to guide the optimal allocation of a given number of monitors. Finally, because the procedure described above actually *generates* $j(t)$, it is useful as a synthesis tool as well – starting with an assumed reference station model we can generate a worst-case input for that station and then verify that the errors due to that input are as predicted.

CONCLUSIONS AND FUTURE WORK

We have presented an algorithm to generate a worst-case bound for differential errors as a function of system parameters for a local area DGPS. The use of one or more reference station monitors reduces the worst-case undetectable error, and a uniform spacing appears to be very nearly optimal in most cases. With further analysis, we should be able to use this metric to derive and specify an optimal monitoring strategy as a function of system parameters for any ground reference station.

Another important direction for future work is the verification of the assumptions used in calculating the various worst-case waveforms discussed here. This verification will be done through software simulation of satellite failure modes and possibly through direct experimentation with some of the hardware components.

ACKNOWLEDGMENTS

The authors would like to thank the Federal Aviation Administration for their generous support of this research. Thanks also to all the members of the Stanford GPS Lab for their insightful comments and suggestions.

REFERENCES

[1] P. Enge, "Local area augmentation of GPS for the precision approach of aircraft," *Proc. IEEE*, vol. 87, pp. 111-132, Jan. 1999.

[2] P. Daly, S. Riley and P. Raby, "Recent advances in the implementation of GNSS," *Proc. ION GPS-93,* Salt Lake City, Utah, 1993.

[3] H. S. Cobb *et. al.,* "Observed GPS signal continuity interruptions," *Proc. ION GPS-95,* Palm Springs, California, 1995.

[4] A. Hansen, T. Walter, P. Enge and D. Lawrence, "GPS satellite clock event on SVN 27 and its impact on augmented navigation systems," Proceedings of ION GPS-98, Nashville, Tennessee, 1998.

[5] R. Williamson, R. Crowell and H. Trotter, *Calculus of Vector Functions.* Prentice-Hall, New Jersey, third edition, pp. 160-166, 1972.

[6] D. Luenberger, *Optimization by Vector Space Methods.* Wiley and Sons, New York, pp. 53-58, 1969.